

ponents have been attributed to a fast, nonergodic decomposition and a slower ergodic reaction both taking place in two steps.³⁵ Transfer of D rather than H has little influence on the relative contributions of the two components in the $C_3H_6O^+$ peak,³⁶ in contrast to the proposal of Holmes and Lossing for 1.

The symmetric ion $CH_3CH_2C(=O^+)CH_2CH_3$ appears to behave ergodically at energies not too far above threshold.^{37,38} Several chemically activated, symmetric neutral species have been shown to behave nonergodically only at very short lifetimes.^{6,7} $CH_3CO_2H^+$ formed from 1 might be more prone to nonergodic behavior than symmetric species because components of the normal modes are identical on opposite sides of symmetric species, while the vibrational motions and frequencies of CH_3 and OH are quite different; this would presumably impede energy transfer between those groups in $CH_3CO_2H^+$. The $SnC_{12}H_{30}F$ radical formed by F addition to gaseous $Sn(CH_2CH=CH_2)_4$ does not achieve energy equilibration across the Sn atom in 10^{-10} – 10^{-9} s.³⁹ The asymmetric ion $CH_3C(=O^+)CH_2CH_3$ may display nonergodic behavior when formed from one or both of the enol isomers.^{40,41}

Nonergodic behavior accompanying chemical reactions is generally thought to be rare.^{42,43} There are two conditions under which nonergodic behavior might accompany chemical reactions: (1) at very short lifetimes,^{6,7} and (2) below a critical internal energy.^{44,45} In most reported examples, nonergodic behavior has been due to very rapid reaction (ca. 10^{-12} s) such that energy randomization does not have the time to occur.^{4,6-8} Following $1 \rightarrow 2$, most ions probably contain at least 15 kJ mol^{-1} more energy

than they need to fragment (Figure 2). At this energy RRKM calculations give an average lifetime of 4×10^{-10} s. This implies that 2 is quite long-lived in comparison to most systems for which nonergodic behavior has been proposed.

The reaction $1 \rightarrow 2 \rightarrow CH_3CO^+ + OH$ may be nonergodic due to an insufficient density of states to permit ergodic behavior. The density of states in 2 at the measured appearance energy for $CH_3CO^+ + OH$ is calculated to be 8×10^3 states per cm^{-1} , while the density of states at the energies at which methyl losses are proposed to show nonergodic behavior probably exceeds 10^6 states cm^{-1} (Figure 3). These results depend on the activation energy for $1 \rightarrow 2$ and assumptions about frequencies used in the calculations. Densities of states for the possible onset of randomization of vibrational energy experimentally observed by others are 10^2 ,⁴⁶ 10^3 ,⁴⁵ and about 3×10^5 ⁴⁷ states per cm^{-1} . Nordholm and Rice⁴⁴ have shown that it is theoretically possible for nonergodic excitation to be followed by nonergodic behavior even above the critical energy for randomization of energy to occur. Ergodic behavior in 1-O-d at higher energies is implied by the nearly identical energy releases in the losses of methyl in collision-induced decompositions of that ion.

Acknowledgment. We thank the Robert A. Welch Foundation (Grants H-609 and A-886) for financial support, Professor Michael Gross and the NSF supported Midwest Center for Mass Spectrometry (Grant 78-18572) for the use of the MS 50 TA, Professor John Holmes for discussion of appearance energy measurements, and Debbie Pavlu, Lisa Kulackoski, and Phyllis Waldrop for typing.

Registry No. 1, 68863-94-5; 1-2-d, 89032-14-4; 1-O,O-d, 89032-15-5; $\cdot CH_2C(OH)OD^+$, 89043-39-0; $CH_3(CH_2)_2CO_2H$, 107-92-6; $CH_3CH_2C-HDCO_2H$, 89032-13-3; $CH_3(CH_2)_2C(O)OD$, 25117-78-6; $CD_3(CH_2)_2CO_2H$, 36789-14-7; $CD_3(CH_2)_2C(O)OD$, 64833-97-2.

(46) Sharp, R. C.; Yablonovitch, E.; Bloembergen, N. *J. Chem. Phys.* **1982**, *76*, 2147.

(47) Reddy, K. V.; Heller, D. F.; Berry, M. J. *J. Chem. Phys.* **1982**, *76*, 14.

- (37) Depke, G.; Schwarz, H. *Org. Mass Spectrom.* **1981**, *16*, 421.
 (38) McAdoo, D. J.; Hudson, C. E. *Org. Mass Spectrom.* **1983**, *18*, 159.
 (39) Rogers, R.; Montague, D. C.; Frank, J. P.; Tyler, S. C.; Rowland, F. *S. Chem. Phys. Lett.* **1982**, *89*, 9.
 (40) Lifshitz, C.; Berger, P.; Tzidony, E. *Chem. Phys. Lett.* **1983**, *95*, 109.
 (41) McAdoo, D. J.; Hudson, C. E. *J. Phys. Chem.* **1983**, *87*, 245.
 (42) Bauer, S. H. *Chem. Rev.* **1978**, *78*, 147.
 (43) Oref, I.; Rabinovitch, B. S. *Acc. Chem. Res.* **1979**, *12*, 166.
 (44) Nordholm, S.; Rice, S. A. *J. Chem. Phys.* **1975**, *62*, 157.
 (45) Smalley, R. E. *J. Phys. Chem.* **1982**, *86*, 3504.

The Chromium Methylidene Cation: $CrCH_2^+$

Emily A. Carter[†] and William A. Goddard III*

Arthur Amos Noyes Laboratory of Chemical Physics,³ California Institute of Technology, Pasadena, California 91125 (Received: October 26, 1983)

We have examined the electronic structure and bonding characteristics of the experimentally observed cation $CrCH_2^+$. We find a 4B_1 ground state with a covalent double bond between $^6S \text{ Cr}^+$ and $^3B_1 \text{ CH}_2$. These results are in contrast to previous theoretical studies which found a lowest state with 6B_1 symmetry and a single Cr–C bond. We calculate a direct bond energy of 44 kcal/mol and estimate the fully correlated limit to be 49 kcal/mol, which may be compared with the experimental value of 65 ± 7 kcal/mol and the previous theoretical results of 18.3 and 22.3 kcal/mol. The differences in results between the two theoretical studies on $CrCH_2^+$ are discussed.

Introduction

Although the bonding and thermodynamic properties of organic molecules are reasonably well understood, little reliable thermochemical information is available for organo-transition-metal complexes. Metal–carbon bond strengths are of particular interest because of the possible role of metal–alkyl, metal–alkylidene, and metal–alkylidene intermediates in the mechanisms of both homogeneous and heterogeneous reactions, e.g., the elucidation of the mechanisms of reductive polymerization of CO by H_2 (Fischer–Tropsch synthesis of hydrocarbons), olefin metathesis by early transition-metal alkylidene complexes, Ziegler–Natta

polymerization of olefins, and many other industrially important catalytic processes.

In the past few years, advances in both theoretical and experimental characterization of metal–carbon species have been attained. GVB calculations of bond energies for several transition-metal alkylidene complexes led to bond strengths of 48–86 kcal/mol.^{1,2} Experimental bond dissociation energies for gas-phase, first-row transition-metal–methylene positive ions, ranging in value from 65 ± 7 to 96 ± 5 kcal/mol, have been determined by Beauchamp and co-workers.³ Schaefer and co-workers have

[†] National Science Foundation Predoctoral Fellow, 1982–85.

^{*} Contribution No. 6936.

(1) Rappé, A. K.; Goddard III, W. A. *J. Am. Chem. Soc.* **1982**, *104*, 448.
 (2) Carter, E. A.; Goddard III, W. A. *Organometallics*, submitted for publication.

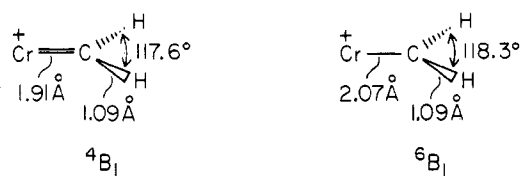


Figure 1. Equilibrium geometries for 4B_1 CrCH_2^+ and 6B_1 CrCH_2^+ .

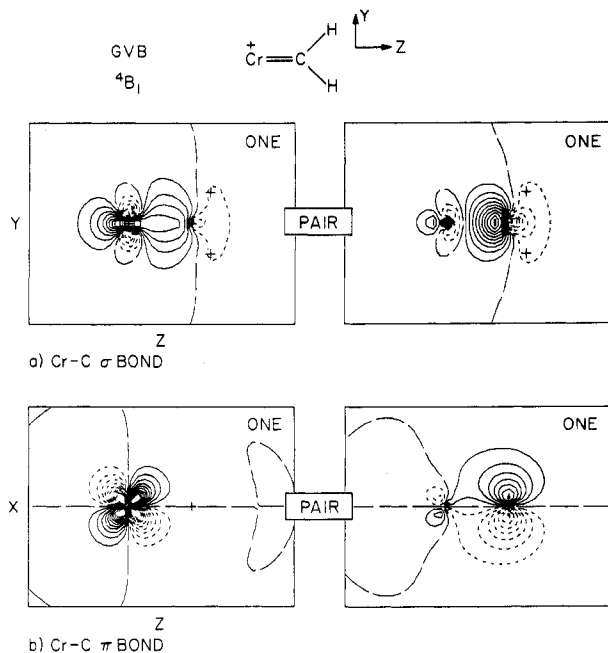
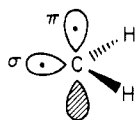


Figure 2. GVB orbitals for 4B_1 CrCH_2^+ at its equilibrium geometry: (a) GVB orbitals for the Cr-C σ bond; (b) GVB orbitals for the Cr-C π bond. Long dashes indicate zero amplitude; the spacing between contours is 0.05 au. The same convention is used in all plots.

carried out Hartree-Fock and configuration interaction calculations on two of the metal-methylene cations observed by Beauchamp, CrCH_2^+ and MnCH_2^+ .⁴ However, the calculations lead to a bond energy of 18.3 kcal/mol for CrCH_2^+ , whereas Beauchamp's result is 65 ± 7 kcal/mol for CrCH_2^+ . (Similarly, for MnCH_2^+ , theory and experiment yield 36.0 and 94 ± 7 kcal/mol, respectively.) The current study was undertaken partly to resolve this large disagreement in bond energies and partly to elucidate the nature of metal-carbon double bonds.

Results and Discussion

Orbitals, Geometry, and Vibrational Frequencies for the Ground State (4B_1). Starting with the ground state of Cr^+ , $(3d)^5$ or 6S , with its five singly occupied orbitals and the ground state (3B_1) of CH_2 with its two singly occupied orbitals (σ, π), we might



expect to find a double bond by simply spin pairing the Cr d_{z^2} orbital with the CH_2 σ orbital and the Cr d_{xz} orbital with the CH_2 π orbital. Indeed, we find the ground state to have exactly this

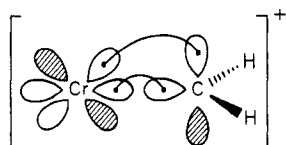


TABLE I: Vibrational Frequencies (cm^{-1}) for 4B_1 and 6B_1 CrCH_2^+ ^a

state	$\nu_{\text{Cr-C}}$	$\nu_{\text{C-H}}$	ν_{HCH} scissors
4B_1	542	3339	1316
6B_1	495	3336	1336

^a Frequencies are calculated from the harmonic force constants obtained from spline fits to $(\text{RCI}^*\text{S})_{\text{valence}}$ calculations.

character, as indicated in Figure 1. Thus the ground state has a Cr-C double bond with orbitals as shown in Figure 2. Each bond pair is quite covalent, involving one electron in an orbital localized on Cr and one electron in an orbital localized on C. Analyzing the orbital character in the Cr σ bond⁵ indicates that although the available σ orbital in the ground state of Cr^+ [$(3d)^5$] is $d\sigma$, the Cr σ orbital of the Cr-C σ bond is 47% 4sp and 53% 3d. The reason for the large amount of s character in the σ bond is analyzed below. As would be expected from these descriptions, we find C_{2v} symmetry (stable with respect to both in-plane and out-of-plane distortions) in the equilibrium geometry for the ground state.

The geometry for this state is given in Figure 1 where we see that the HCH bond angle is identical with that in ethylene (117.6°). The calculated Cr=C bond length (1.91 Å) cannot be directly compared with experiment since no chromium-alkylidene complexes have been structurally characterized. The Cr-C bond length may be compared with theoretical values for MnCH_2^+ [$R(\text{Mn}=\text{C}) = 2.01$ Å] and FeCH_2^+ [$R(\text{Fe}=\text{C}) = 1.96$ Å].⁶ The Mn-C bond is substantially longer than the Cr-C bond because Mn(I) bonds to CH_2 in its $(4s)^1(3d)^5$ ground state, using the larger 4s orbital to make the σ bond and a 3d orbital to make the π bond, whereas the σ bond in CrCH_2^+ is only 47% sp and hence is much smaller than in MnCH_2^+ . For the same reason, a $\text{Cr}^0=\text{CH}_2$ (s^1d^5 Cr) would have a much longer bond (the σ bond would involve primarily the 4s orbital on Cr) than our $\text{Cr}^1=\text{CH}_2$, whereas a $\text{Cr}^{II}=\text{CH}_2$ (d^4 Cr^{2+}) complex should have a much shorter bond (since the σ bond would involve a pure Cr 3d orbital).

The vibrational frequencies for both the 4B_1 ground state and the 6B_1 excited state are listed in Table I. To our knowledge, no experimental metal-carbon double bond vibrational frequencies have been reported; however, these values (542 and 495 cm^{-1}) can be compared with calculations on $\text{ClRuH}(\text{CH}_2)$, where the Ru-C stretching frequencies were calculated to be 746 and 798 cm^{-1} for the two states examined.² Given the much stronger bond strength in the Ru complex (91 kcal) compared with the Cr system (49 kcal), coupled with similar M-C distances, leads to the prediction of a higher vibrational frequency in the Ru system, as observed. The C-H stretching frequencies (3339 and 3336 cm^{-1}) are a bit high when compared with the C-H stretch in $\text{CH}_2=\text{CH}_2$ (3056 cm^{-1}). However, Schaefer has noted that theoretical X-H vibrational frequencies are generally high by 10%.⁷ The H-C-H scissors mode (1316 and 1336 cm^{-1}) is similar to the value for the same mode in ethylene (1393 cm^{-1}), as expected for an H-C-H bend of an sp^2 -hybridized center.

The Sextet Excited State (6B_1). As discussed below, the sextet ground state of Cr^+ results from the large number of (negative) exchange interactions engendered by this high spin state (the basis of Hund's rule). Spin pairing of the CH_2 and Cr^+ orbitals has the effect of decreasing this exchange stabilization, and thus for sufficiently small overlap, bond pairing will not be able to overcome the spin stabilization. Thus we find a low-lying excited state consisting of a σ bond (CH_2 σ with Cr d_{z^2}) but no π bond. In this case the CH_2 π orbital is coupled high spin with the remaining four Cr d orbitals to yield an $S = 5/2$ or sextet state (6B_1). The geometry for the 6B_1 state is shown in Figure 1. The Cr-C bond length has increased from 1.91 to 2.07 Å, as expected from the

(5) Analyses of orbital character in the GVB orbitals are carried out by summing over Mulliken populations for the first and second NO's of each GVB pair.

(6) Brusich, M. J.; Goddard III, W. A., to be submitted for publication.

(7) Schaefer III, H. F. "The Electronic Structure of Atoms and Molecules"; Addison-Wesley: Reading, MA, 1972.

(3) Armentrout, P. B.; Halle, L. F.; Beauchamp, J. L. *J. Am. Chem. Soc.* **1981**, *103*, 6501.

(4) Vincent, M. A.; Yoshioka, Y.; Schaefer III, H. F. *J. Phys. Chem.* **1982**, *86*, 3905.

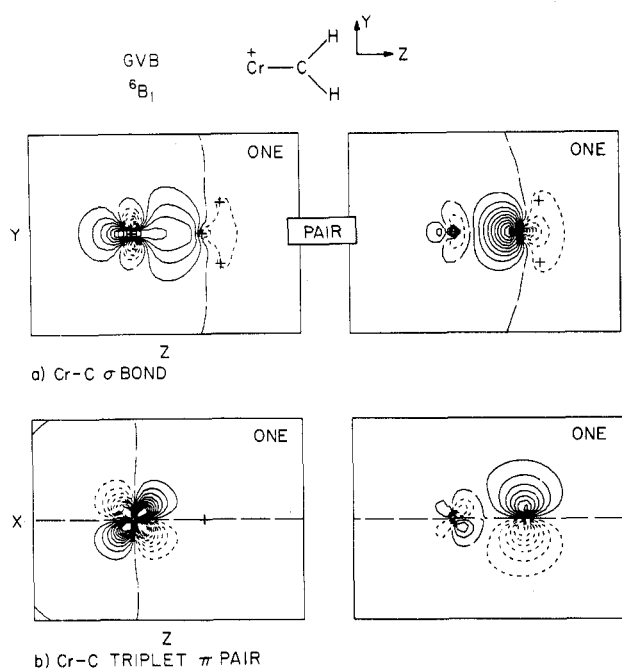


Figure 3. GVB orbitals for 6B_1 CrCH_2^+ at its equilibrium geometry: (a) GVB orbitals for the Cr-C σ bond; (b) GVB orbitals for the Cr-C π bond.

TABLE II: d-d and s-d Exchange Integrals^a for Cr^+ (kcal/mol)

state	K_{sd}	K_{dd}
6S (d^5)		16.5
6D (s^1d^4)	5.0	18.4

^a Averaged over the various d orbitals.

repulsion induced by triplet coupling of the π electron pair. The C-H bond length and the H-C-H angle are approximately the same for both states, indicating that the hybridization of the carbon orbitals has not changed. We find C_{2v} symmetry for the equilibrium geometry of the 6B_1 state, again stable with respect to in-plane and out-of-plane distortions. The Cr-C bonding orbitals for the sextet state are shown in Figure 3. Again, the Cr-C σ bond is quite covalent, with one electron in a Cr d orbital and one electron in a C sp hybrid orbital. The triplet-coupled π orbitals of the sextet state look similar to the π pair in the quartet state, except that the triplet π orbitals must get orthogonal to one another, as evidenced from the node around Cr built into the carbon p π orbital.

Exchange Couplings. Before proceeding, it is appropriate to be a bit more explicit about the role of exchange interactions in Cr^+ and CrCH_2^+ . Cr^+ has a high-spin, $(3d)^5$, 6S ground state and a high-spin, $(4s)^1(3d)^4$, 6D first excited state which lies 1.52 eV (35.1 kcal/mol higher in energy).⁸ The 6S state is lower than the 6D state because the magnitude of the exchange terms is larger for the high-spin d^5 case. The 6S state has ten d-d exchange terms (K_{dd}) between the five d electrons, whereas the 6D has six K_{dd} and four K_{sd} terms between the four d electrons and the s electron.

$$E_{\text{ex}}(d^5) = -10K_{dd}$$

$$E_{\text{ex}}(s^1d^4) = -6K_{dd} - 4K_{sd}$$

The d-d exchange terms are larger than the s-d exchange terms (see Table II), leading to a larger overall exchange energy contribution in the 6S state.

Using the average d-d and d-s exchange terms from Table II, we can now predict the nature of the bonding in CrCH_2^+ . Indeed, analyzing the differential loss of exchange terms (see Figure 4) expected upon bonding CH_2 to Cr^+ in either the $(3d)^5$ ground state or the $(4s)^1(3d)^4$ excited state allows a prediction of the fraction

4B_1 CrCH_2^+ : LOSS OF EXCHANGE UPON BONDING

Cr^+ (s^1d^4)			Cr^+ (d^5)		
Cr-C σ BOND: pure Cr 4s σ			Cr-C σ BOND: pure Cr 3d σ		
Cr-C π BOND: pure Cr 3d π			Cr-C π BOND: pure Cr 3d π		
	Cr^+	CH_2		Cr^+	CH_2
4s σ	$\left\{ \begin{array}{l} 1/2 \text{ } \uparrow \text{ } \uparrow \\ 1/2 \text{ } \uparrow \text{ } \uparrow \end{array} \right\}$	$2sp\sigma$	4s σ	—	
3d σ	—		3d σ	$\left\{ \begin{array}{l} 1/2 \text{ } \uparrow \text{ } \uparrow \\ 1/2 \text{ } \uparrow \text{ } \uparrow \end{array} \right\}$	$2sp\sigma$
3d π_x	$\left\{ \begin{array}{l} 1/2 \text{ } \uparrow \text{ } \uparrow \\ 1/2 \text{ } \uparrow \text{ } \uparrow \end{array} \right\}$	$2p\pi$	3d π_x	$\left\{ \begin{array}{l} 1/2 \text{ } \uparrow \text{ } \uparrow \\ 1/2 \text{ } \uparrow \text{ } \uparrow \end{array} \right\}$	$2p\pi$
3d π_y	\uparrow		3d π_y	\uparrow	
3d δ_{xy}	\uparrow		3d δ_{xy}	\uparrow	
3d $\delta_{x^2-y^2}$	\uparrow		3d $\delta_{x^2-y^2}$	\uparrow	
$K_{dd}^{\text{Cr}^+}$	-6	-4.5	$K_{dd}^{\text{Cr}^+}$	-10	-6.5
$K_{sd}^{\text{Cr}^+}$	-4	-2	ΔK^{Cr^+}	0	0
		+1.5			+3.5
		+2			0

$K_{dd}^{\text{Cr}^+}$ = Number of exchange terms (K_{dd} and K_{sd}) for Cr^+ before bonding to CH_2 .

$K_{sd}^{\text{Cr}^+}$ = Number of exchange terms (K_{dd} and K_{sd}) for Cr^+ after bonding to CH_2 .

ΔK^{Cr^+} = Differential loss of exchange for Cr^+ upon bonding to CH_2 .

Figure 4. Diagram depicting the origin of the differential loss of exchange upon bonding CH_2 to a $4s\sigma/3d\pi$ combination or to a $3d\sigma/3d\pi$ combination on Cr.

TABLE III: 6B_1 - 4B_1 Excitation Energies for CrCH_2^+ ^a

calculations	(4B_1), no. config/ no. SEF ^b	(6B_1), no. config/ no. SEF	ΔE - (6B_1), kcal	ground state
HF	1/1	1/1	-53.7	6B_1
GVB-PP	4/4	2/2	-11.3	6B_1
GVB-RCI	9/34	5/10	+12.5	4B_1
(GVB-RCI*S) _{valence}	507/3912	327/1501	+18.0	4B_1
RCI π *D σ +RCI σ *D π +(RCI*S) _{valence}	1415/8928	482/2146	+19.0	4B_1

^a The geometries used were the optimum values calculated at the (GVB-RCI*S)_{valence} level. ^b no. config = number of spatial configurations. SEF = spin eigenfunctions.

of 4s and 3d character in the Cr-C σ bond. Pairing the orbitals of Cr^+ and CH_2 into a simple, doubly bonded 4B_1 state for CrCH_2^+ leads to a loss of favorable (negative) exchange terms due to spin pairing in the bond.⁹ If both the Cr-C bonds are to Cr d orbitals, $3.5K_{dd}$ are lost upon bonding (57.8 kcal/mol). If the σ bond involves the Cr 4s orbital instead of a 3d orbital, $1.5K_{dd}$ and $2K_{sd}$ are lost (27.6 kcal/mol). Thus it is intrinsically (30.2 kcal/mol) more favorable to bond methylene to one Cr s orbital and one Cr d orbital than to two Cr d orbitals. However, the excitation energy to the $(4s)^1(3d)^4$ state of Cr^+ is 33.9 kcal/mol.¹⁰ Thus one expects an almost 50/50 mix of s and d (instead of pure d) in the σ orbital, as observed.

6B_1 - 4B_1 State Splitting: The Importance of Correlation. The energy difference between the sextet state and the quartet state

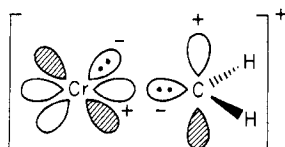
(9) This simple analysis is true only for perfect singlet pairing in each bond. If we include other spin-coupling terms (e.g., in an RCI wave function), we gain back some of the exchange energy we lose by singlet pairing each bond pair, complicating the hybridization analysis.

(10) Our calculations on Cr^+ lead to 33.9 kcal/mol as the state splitting for $\text{Cr}^+(d^5)$ - $\text{Cr}^+(s^1d^4)$. The experimental result is 35.1 kcal/mol, averaged over total angular momentum states. See ref 8.

(8) Moore, C. E. *Natl. Stand. Ref. Data Sec., Natl. Bur. Stand.* 1971, No. 35, Vol. 2, p 10.

as a function of the level of electron correlation is given in Table III. Note that Hartree-Fock prefers the 6B_1 state by 54 kcal, whereas the basic GVB description (GVB-RCI, including the spin-coupling configurations) leads to a 4B_1 ground state by 12.5 kcal. The highest level calculated leads to a 4B_1 ground state by 19.0 kcal. Why is there such a dramatic effect of electron correlation upon the stability of these spin states? In Brooks and Schaefer's previous work on $MnCH_2$,¹¹ Hund's rules were assumed valid for these systems, which would then suggest a sextet ground state for $CrCH_2^+$. However, Hund's rules only apply in cases of *mutually orthogonal* orbitals, where the exchange terms necessarily favor a high-spin ground state. For orbitals that overlap, one-electron terms generally dominate exchange terms, so that low-spin ground states are expected. Thus the 4B_1 state is the expected ground state for $CrCH_2^+$.

Why does Hartree-Fock theory not lead to the correct ground state? The reason is that Hartree-Fock cannot describe the doubly bonded state properly. This state involves a π bond with low overlap ($S_{Cr-C\pi} = 0.33$), whereas in Hartree-Fock the two orbitals in the bond pair must have unit overlap. To resolve this conflict, the optimum Hartree-Fock orbitals become very ionic (π electrons on the metal; σ electrons on the CH_2) so as to be consistent with the doubly occupied orbitals. This charge separation is highly



unfavorable, forcing the Hartree-Fock 4B_1 state very high in energy. On the other hand, for the 6B_1 state, triplet pairing of the Cr π_x and C π_x electrons forces these π electrons to be in separate, mutually orthogonal orbitals. To whatever the CH_2 π_x and Cr π_x atomic orbitals overlap, there will be an antibonding interaction. However, for ${}^+Cr-CH_2$ this overlap is small so that Hartree-Fock predicts a high-spin ground state, with a single Cr-C σ bond.

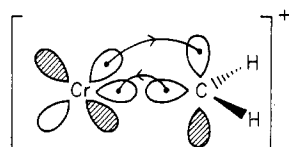
In the GVB wave function, we allow the two orbitals of each pair to have their optimum overlap, removing the restriction that causes Hartree-Fock to yield an ionic description of the π bond for the 4B_1 state. For a purely covalent bond, the GVB wave function would have the form $\Psi = lr + rl$, except that the GVB wave function allow l and r to have whatever shape minimizes the energy of the wave function.

$$\psi_{HF} = \phi_a \phi_a$$

$$\psi_{covalent} = \phi_l \phi_r + \phi_r \phi_l$$

$$\psi_{GVB} = \phi_a \phi_b + \phi_b \phi_a$$

Generally the optimum wave function is about $\sim 90\%$ covalent and $\sim 10\%$ ionic. In the GVB wave function for a double bond, there are two possible spin couplings (VB structures) that should be optimized along with the orbitals. However, for computational convenience, we generally optimize the orbitals only for one structure (perfect pairing), leading to the GVB-PP wave function. These spin coupling terms are then included by a CI in which the two electrons in each pair are allowed to have all three possible occupations of the two orbitals for that pair. This wave function, the GVB-RCI, has nine spatial configurations for a double bond. In addition to the GVB spin coupling, this wave function allows for interpair correlation and atomic high-spin coupling. The interpair correlation allows for correlated movement of electrons in one pair to one side of a bond, while electrons in another pair move to the other side of a bond, for an overall covalent structure:

TABLE IV: Cr-C Bond Energies (kcal/mol) of $CrCH_2^+$

calculation	4B_1 state		6B_1 state	
	total energy, hartree	bond energy	total energy, hartree	bond energy
HF	-1 080.829 94	-60.9	-1 080.915 49	-7.2
GVB(2/4)-PP	-1 080.915 49	-7.2	-1 080.933 53	+4.1
GVB-RCI	-1 080.956 18	+18.3	-1 080.936 22	+5.8
RCI $_{\pi}^*D_{\sigma} +$	-1 080.983 98	+35.8		
RCI $_{\sigma}^*D_{\pi}$				
(RCI *S) $_{valence}$	-1 081.000 43	+38.8	-1 080.971 67	+20.8
RCI $_{\pi}^*D_{\sigma} +$	-1 081.008 68	+44.0	-1 080.978 39	+25.0
RCI $_{\sigma}^*D_{\pi} +$				
(RCI *S) $_{valence}$				

The RCI wave function allows the Cr d electrons in bond pairs to gain back some of the exchange energy they have lost in bonding by including the atomic high-spin coupling. These spin-coupling effects are expected to be more important for the 4B_1 state than for the 6B_1 state, since more exchange terms are lost by bond pairing two Cr orbitals to CH_2 to form a double bond instead of a single bond. The 6B_1 state gains little back from atomic high-spin coupling since it already has five electrons high-spin coupled. Thus the major element that brings about the inversion of ground states is including optimal spin coupling in the GVB wave function. Allowing Cr to have both favorable exchange interactions as well as favorable bonding interactions results in the doubly bonded 4B_1 ground state for $CrCH_2^+$.

Bond Energies. Calculating the Cr-C bond strength dissociation consistently¹² (vide infra) leads to a direct bond energy of 44.0 kcal/mol for 4B_1 $CrCH_2^+$, dissociating into ground-state fragments, 6S Cr $^+$ and 3B_1 CH_2 . An indication of the importance of electron correlation in transition-metal systems is exhibited in Table IV. As the level electron correlation accounted for increases, so does the bond energy, as expected when a more accurate description of the bound molecule is obtained.

All bond energies for $CrCH_2^+$ are calculated in a "dissociation-consistent" manner. This means that we calculate a wave function at $R_e(Cr-C)$ which smoothly dissociates to the proper covalent limits at $R(Cr-C) = \infty$, retaining the same description of electron correlation in the wave function for $R = \infty$ that existed for R_e . Thus our bond energies are said to be "dissociation-consistent".

Such dissociation-consistent wave functions should be expected to yield bond energies that are too small, although the bond energies will increase as the level of electron correlation is increased. In order to estimate the role of reduced correlation energy at our best level of calculation, we will compare the results of the same calculational level on a known bond energy of CH_2 , namely, in $H_2C=CH_2$. The results for various levels of dissociation-consistent calculations on ethylene (using the same bases as for $CrCH_2^+$) are shown in Table V. Using the same basis set for carbon and hydrogen as was used for the $CrCH_2^+$ calculations (vide infra) and the same level of dissociation-consistent CI leads to a direct bond energy for $CH_2=CH_2$ of $D_e = 175.4$ kcal/mol as compared with the experimental value of 180.0 kcal/mol. This 4.6 kcal/mol of residual correlation energy for $CH_2=CH_2$ is expected to be a lower bound on the residual error in our calculation of the $CrCH_2^+$ bond energy (since Cr may have additional correlation errors from the other Cr d orbitals). Thus, our best (probably conservative) estimate for the bond energy for $CrCH_2^+$ is $D_e = 48.6$ kcal/mol.

Comparisons with Previous Theoretical Studies. Vincent et al.⁴ carried out Hartree-Fock calculations on the 6B_1 state, leading to an optimum geometry with $R_{Cr-C} = 2.064$ Å and $\theta_{H-C-H} = 113.5^\circ$, whereas using correlated wave functions we find $R_{Cr-C} = 1.91$ Å and $\theta_{H-C-H} = 117.6^\circ$ for the 4B_1 state and $R_{Cr-C} = 2.07$ Å and $\theta_{H-C-H} = 118.3^\circ$ for the 6B_1 state. The smaller θ_{H-C-H} in the Hartree-Fock geometry is indicative of a larger amount of

(11) Brooks, B. R.; Schaefer III, H. F. *Mol. Phys.* 1977, 34, 193.(12) Bair, R. A.; Goddard III, W. A. *J. Phys. Chem.*, submitted for publication. See Bair, R. A. Ph.D. Thesis, California Institute of Technology, June 1981.

TABLE V: C-C Bond Energies for Ethylene (kcal/mol)

calculation	total energy, hartree		no. config/SEF ^a		D _e (CH ₂ =CH ₂)	
	VDZ ^b	VDZd ^c	VDZ	VDZd	VDZ	VDZd
HF	-78.011 30	-78.040 81 ^d	1/1	1/1	115.7	122.8 ^d
GVB(2/4)-PP	-78.051 39	-78.079 57 ^e	4/4	4/4	140.8	147.0 ^e
GVB-RCI(4)	-78.066 51	-78.092 50 ^d	5/6	5/6	150.3	155.3 ^d
(GVB-RCI*S) _{valence}	-78.096 61	-78.130 16 ^d	167/292	263/460	160.2	164.2 ^d
D _π *RCI _σ + D _σ *RCI _π + (RCI*S) _{valence} expt	-78.101 80	-78.148 01 ^e	367/544	759/1096	163.4	175.4 ^e 180.0 ^f

^a Given for CH₂=CH₂ only. ^b VDZ = valence double ζ bases for C and H. Reference 18. ^c VDZd = VDZ + one set of C d polarization functions. ^d Reference 6. ^e This work. Reference 19. ^f "JANAF Thermochemical Tables", *Natl. Stand. Ref. Data Sec., Natl. Bur. Stand.* 1970, No. 37.

TABLE VI: Davidson's Correction for ⁴B₁ and ⁶B₁ CrCH₂⁺

state	limit of CI ^a	no. config/SEF	total energy, hartree	quadruples contribn, kcal/mol	Davidson's cor, kcal/mol
⁴ B ₁	doubles	502/2197	-1 080.984 89		12.1
⁴ B ₁	quadruples	1373/8829	-1 081.008 61	14.9	
⁴ B ₁	unlimited	1415/8928	-1 081.008 68		
⁶ B ₁	doubles	320/1699	-1 080.977 70		2.2
⁶ B ₁	quadruples ^b	482/2146	-1 080.978 39	0.4	

^a The "unlimited" CI is our dissociation-consistent D_π*RCI_σ + D_σ*RCI_π + (RCI*S)_{valence}. This CI is then limited to doubles or quadruples. ^b "Quadruples" is the same as the unlimited CI in this orbital space.

¹A₁ character in the CH₂ part of the wave function ($\theta^{\text{opt}} = 104^\circ$) as opposed to ³B₁ character ($\theta^{\text{opt}} = 133^\circ$).

At the optimum Hartree-Fock geometry, Vincent et al. carried out a singles and doubles CI (SD-CI) calculation leading to a bond energy of 18.3 kcal/mol. Including Davidson's correction¹³ for quadruple excitations yielded a bond energy of 22.3 kcal/mol. Since Davidson's correction is only an estimate, we decided to test the calculation of the quadruples correction by carrying out our best level of calculation restricted first to doubles and then to quadruples to directly calculate the correlation energy gained by including excitations up to quadruples. The results are shown in Table VI. Davidson's correction was also calculated from the formula, $\Delta E_Q = (1 - C_0^2)\Delta E_D$ (where C₀ refers to the CI coefficient for the dominant configuration in the singles and doubles CI calculation, ΔE_D is the difference in total energies of the SCF wave function—in this case a GVB-PP wave function—and the singles and doubles CI wave function, and ΔE_Q is the estimated difference in the total energies of the SD-CI wave function and the wave function that includes up through quadruple excitations). By knowing C₀ and ΔE_D , we have calculated ΔE_Q for comparison with the ab initio "Davidson's correction". The results show that Davidson's formula underestimates the amount of correlation for low-spin states and overestimates the correlation error for high-spin states. Thus, the Vincent et al. estimate of the bond energy in ⁶B₁ CrCH₂⁺ may be slightly high, due to an overestimate of Davidson's correction. Perhaps a more accurate estimate of their bond energy would be 18.3 (SD-CI result) + 0.4 = 18.7 kcal/mol.

Vincent et al. also carried out Hartree-Fock calculations on the ⁴B₁ state; however, the ⁴B₁ state is not bound in this description. The major problem here is that the Hartree-Fock description of the ⁴B₁ state is extremely high in energy (54 kcal above ⁶B₁) with quite distorted orbitals (see Figure 5). The Hartree-Fock σ MO is localized primarily on the CH₂ ligand, while the Hartree-Fock π MO is localized primarily on Cr, with a small amount of delocalization onto the CH₂ ligand. Thus the Hartree-Fock description is not a covalent description where each bond has one electron localized near each nucleus. Even with HFSD-CI, the ⁴B₁ state is not bound. Thus double excitations are not sufficient both to change the shape of the orbitals and to include correlation effects. Starting with a Hartree-Fock wave function, we should include at least triple excitations and preferably quadruple excitations in order to get a description comparable to GVB. The strength of the GVB approach is that the correlation effects are

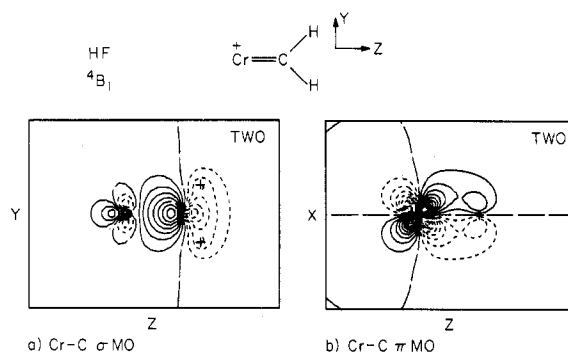
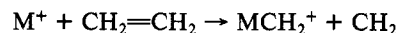


Figure 5. Hartree-Fock orbitals for ⁴B₁ CrCH₂⁺ at its equilibrium geometry: (a) the Cr-C σ bond; (b) the Cr-C π bond.

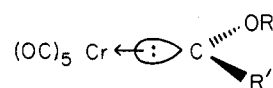
included self-consistently so that the orbital shapes are optimum for various electron correlation terms. This allows a small CI to obtain a high-quality result.

Comparison with Experiment. Experimental bond energies for metal-carbon doubly bonded species have only recently become available through the ion beam studies by Beauchamp and co-workers.³ The bond energies were determined from measuring the reaction cross section for the reaction of CH₂=CH₂ with first-row transition-metal ions.



Although these values are for isolated gas-phase ions, they have provided the only clue into a thermochemical description of solution organometallic chemistry. Beauchamp and co-workers have determined M=CH₂⁺ bond strengths for Cr⁺ through Ni⁺ that range from 65 to 96 kcal/mol, with $D(\text{Cr}=\text{C}) = 65 \pm 7$ kcal/mol. The weak point of the ion beam technique is lack of structural information. It is not possible to decide between two isomeric structures. Our results suggest a weaker bond energy (49 kcal) for Cr⁺=CH₂; however, it is conceivable that another isomer could have a stronger bond.

As mentioned previously, there are no examples of structurally characterized chromium-alkylidene complexes with which to compare. Fischer has characterized chromium singlet carbene complexes with typical Cr-C bond lengths of 2.00–2.15 Å,¹⁴



(13) (a) Davidson, E. R. In "The World of Quantum Chemistry"; Daudel, R.; Pullman, B., Eds.; Reidel: Dordrecht, Holland, 1974; p 17. (b) Langhofs, S. R.; Davidson, E. R. *Int. J. Quant. Chem.* 1974, 8, 61.

(14) Fischer, E. O. *Pure Appl. Chem.* 1972, 30, 353.

somewhat longer than the results presented above. However, since Fischer carbenes have a single dative bond from a doubly occupied σ orbital on the carbene ligand, they are expected to have longer bonds than those found for doubly bonded Cr–C systems. Most known metal–alkylidene complexes are found among third-row transition metals. Two examples of third-row, terminal alkylidene complexes are Schrock's $\text{Cp}_2\text{Ta}(\text{CH}_2)\text{CH}_3$ ($\text{Cp} = \eta^5\text{-C}_5\text{H}_5$) with a Ta–CH₂ bond length of 2.03 Å¹⁵ and $\text{W}(\text{O})(\text{CHCM}_3)(\text{PEt}_3)\text{Cl}_2$ with a W–CH₂ bond length of 1.88 Å.¹⁶ Both systems are expected to have $\text{M}=\text{CH}_2$ double bonds with primarily d character in the σ bond. As a result, the $\text{W}=\text{C}$ bond is shorter than our Cr=C bond!

Summary. We find that the ground state of CrCH_2^+ consists of a covalent Cr–C double bond, where the Cr–C σ bond has nearly equal parts 4s and 3d character. The hybridization and nature of the ground state has been explained in terms of differential changes in exchange terms, K_{dd} and K_{sd} . The ${}^6\text{B}_1$ – ${}^4\text{B}_1$ energy difference as a function of correlation has been discussed. In addition, we find a direct bond energy of 44 kcal and an estimated bond energy of 48.6 kcal/mol, in fair agreement with experiment, 65 ± 7 kcal.

Computational Details

Basis Sets. We explicitly considered all electrons for Cr, C, and H. We used a valence double ζ basis for Cr (10s8p5d/5s4p2d)¹⁷ and the Dunning–Huzinaga valence double ζ bases for carbon (9s5p/3s2p) and for hydrogen (4s/2s).¹⁸ One set of d polarization functions was added to the carbon basis, optimized for CrCH_2^+ ($\zeta = 0.69$).¹⁹

Wave Functions. The geometry optimizations for both the ${}^6\text{B}_1$ and ${}^4\text{B}_1$ states of CrCH_2^+ were carried out by utilizing a (GVB-RCI*S)_{valence} wave function (generalized valence bond restricted configuration interaction times singles from all valence orbitals).

(a) For the ${}^4\text{B}_1$ state, the GVB(2/4) wave function corresponds to correlating the Cr–C σ and Cr–C π bond, each with a second natural orbital, leading to four natural orbitals in all. The C–H pairs were left uncorrelated but solved for self-consistently. The RCI allows all configurations arising from different occupations of each pair of natural orbitals for each GVB bond pair ($3^2 = 9$ spatial configurations and 34 spin eigenfunctions), allowing for interpair correlation and GF coupling. Then we allow all single excitations from all valence orbitals of the nine spatial configurations of the RCI wave function to all virtual orbitals (this includes single excitations from the CH pairs and the singly occupied Cr d orbitals), for a total of 507 spatial configurations and 3912 spin eigenfunctions. The single excitations allow for orbital readjustment upon stretching or bending the molecule.

(b) For the ${}^6\text{B}_1$ state, the GVB(1/2) wave function corresponds to correlating the Cr–C σ bond pair with a second natural orbital, while the Cr–C π system is described by two high-spin-coupled orbitals. This is comparable to the GVB(2/4) wave function for the ${}^4\text{B}_1$ state. Both have four valence orbitals, with two Cr–C σ natural orbitals and two Cr–C π natural orbitals. The RCI

allows all single and double excitations within the GVB σ pair and within the two singly occupied Cr–C π natural orbitals (the valence bond orbitals that compose the π bond in the ground state, ${}^4\text{B}_1$), resulting in five spatial configurations and ten spin eigenfunctions. For the GVB-RCI*S wave function, we start with each of the five spatial configurations of the RCI wave function and allow all single excitations from all valence orbitals to all virtual orbitals, for a total of 327 spatial configurations and 1501 spin eigenfunctions.

To calculate the Cr–C bond energy in CrCH_2^+ , we used several different dissociation-consistent CI¹² wave functions at the equilibrium geometries of CrCH_2^+ and of ${}^3\text{B}_1 \text{CH}_2$ [$\theta_{\text{H-C-H}} = 133^\circ$, $R(\text{C-H}) = 1.078 \text{ \AA}$].²⁰ In addition to calculating the Cr–C bond energy at the HF level,²¹ the GVB-PP (generalized valence bond with perfect pairing restriction) level, the GVB-RCI level (vide supra), and the (GVB-RCI*S)_{valence} level (vide supra), we also carried out two further dissociation-consistent CI's on the ${}^4\text{B}_1$ ground state and one further dissociation-consistent CI on the ${}^6\text{B}_1$ excited state.

(a) $\text{RCI}_\pi^* \text{D}_\sigma + \text{RCI}_\sigma^* \text{D}_\pi$: This CI (for ${}^4\text{B}_1 \text{CrCH}_2^+$ only) consists of all single and double excitations from the three RCI configurations of the Cr–C σ bond pair, simultaneous with an RCI in the Cr–C π bond pair plus the opposite—all singles and doubles from the Cr–C π bond RCI configurations, simultaneous with an RCI in the Cr–C σ bond pair. Note the excitations are from the Cr–C bond pairs to all virtuals, including excitations to Cr singly occupied d orbitals and to the other GVB pair. This leads to a total of 1025 spatial configurations and 5810 spin eigenfunctions for the ${}^4\text{B}_1$ state (note that this includes the generic "GVB-CI" configurations). This wave function dissociates correctly to HF fragments, ${}^6\text{S Cr}^+$ and ${}^3\text{B}_1 \text{CH}_2$.

(b) $\text{RCI}_\pi^* \text{D}_\sigma + \text{RCI}_\sigma^* \text{D}_\pi + (\text{RCI}^* \text{S})_{\text{valence}}$: This CI wave function includes all the configurations for the wave function described directly above, but, in addition, includes the RCI*S configurations (same as described for the geometry optimization) not present in the previous wave function, leading to 1415 spatial configurations and 8928 spin eigenfunctions for the ${}^4\text{B}_1$ state and 482 spatial configurations and 2146 spin eigenfunctions for the ${}^6\text{B}_1$ state. This wave function correctly dissociates to HF*S (all single excitations from the HF wave function) fragments.

The C–C bond energy of ethylene was calculated at the HF, GVB(2/4)-PP, GVB-RCI(4), (GVB-RCI*S)_{valence}, and $\text{RCI}_\pi^* \text{D}_\sigma + \text{RCI}_\sigma^* \text{D}_\pi + (\text{RCI}^* \text{S})_{\text{valence}}$ levels, as described above, using VDZ bases for C and H.¹⁸ The effect of C d functions on the C–C bond energy was examined by using the d function optimized for CrCH_2^+ .¹⁹ The ${}^3\text{B}_1 \text{CH}_2$ fragment was calculated at the equilibrium geometry ($\theta = 133^\circ$, $R(\text{C-H}) = 1.078 \text{ \AA}$)²⁰ at the HF and HF*S levels.

The ${}^6\text{B}_1$ – ${}^4\text{B}_1$ state splittings were calculated by using all of the above methods. The ${}^6\text{D}$ – ${}^6\text{S}$ state splittings for Cr^+ were calculated at the Hartree–Fock level, using an averaged-field Hamiltonian to represent the four d electrons in ${}^6\text{D Cr}^+$. The exchange integrals for ${}^6\text{D Cr}^+$ and ${}^6\text{S Cr}^+$ were taken from Hartree–Fock calculations.

Acknowledgment. This work was supported in part by grants from the National Science Foundation (No. DMR82-15650) and the Shell Development Company.

Registry No. CrCH_2^+ , 88968-58-5.

(20) Shih, S.-K.; Peyerimhoff, S. D.; Buenker, R. J.; Peric, M. *Chem. Phys. Lett.* **1978**, *55*, 206.

(21) Although Hartree–Fock does not dissociate correctly, we include this calculation for completeness.

(15) Guggenberger, L. J.; Schrock, R. R. *J. Am. Chem. Soc.* **1975**, *97*, 6578.

(16) Wengrovius, J. H.; Schrock, R. R.; Churchill, M. R.; Missert, J. R.; Youngs, W. J. *J. Am. Chem. Soc.* **1980**, *102*, 4515.

(17) Rappé, A. K.; Goddard III, W. A., unpublished results. See, for example, Rappé, A. K.; Smedley, T. A.; Goddard III, W. A. *J. Phys. Chem.* **1981**, *85*, 2607.

(18) Huzinaga, S. *J. Chem. Phys.* **1965**, *42*, 1293. Dunning, Jr., T. H. *Ibid.* **1970**, *53*, 2823.

(19) The C d function ($\zeta = 0.69$) was optimized by using a fixed geometry [$R(\text{Cr-C}) = 2.10 \text{ \AA}$, $\theta_{\text{H-C-H}} = 120^\circ$, $R(\text{C-H}) = 1.078 \text{ \AA}$] at the RCI*S level.